BACKLASH GAP POSITION ESTIMATION IN AUTOMOTIVE POWERTRAINS

Adam Lagerberg*, Bo S. Egardt†

* School of Engineering, Jönköping University, P.O. Box 1026, SE-551 11 Jönköping, Sweden,
adam.lagerberg@ing.hj.se, Fax: +46-36 34 04 84
† Chalmers University of Technology, SE-412 96 Gothenburg, Sweden,
egardt@s2.chalmers.se, Fax: +46-31 772 3730

Keywords: Backlash, Estimation, Event based sampling, Extended Kalman filter, Automotive applications.

Abstract

Backlash in automotive powertrains is a major source of driveability limitations. In order to increase the powertrain controller performance, knowledge of the backlash properties (size and current position) is needed. In this paper, a nonlinear estimator for the current angular position in the backlash is developed, based on extended Kalman filtering theory. A linear estimator for fast and accurate estimation of the angular position of a wheel and the engine is also described. It utilizes standard ABS sensors and engine speed sensors, and is based on event based sampling, at each pulse from the sensors. The results show that the backlash position estimate is of high quality, and robust to modeling errors. The performance is increased further when the event based position estimators are used as pre-filters.

1 Introduction

Backlash is always present in an automotive powertrain, and it causes problems with driveability of the vehicle. Therefore, engine control systems must compensate for the backlash [2], [7]. In order to design a powertrain control system with high performance, the current position in the backlash is an important input signal [8].

In this paper, estimators for the position in the backlash and the total shaft displacement is described. The position difference between wheels and engine comes from the powertrain backlash and from the shaft twist due to flexibility. The principle is to estimate these contributions based on position information from wheel and engine sensors. The engine control signal is also used. The estimators are based on the Kalman filter theory.

Speed and acceleration estimation by Kalman filters in backlash-free rotating systems were treated in [4] and [14]. In [5] the size of the backlash was estimated together with the shaft stiffness for an industrial robot arm. In [10, 11] the backlash size in an industrial drive system was estimated. In these papers, the current position was however not estimated. The focus in this paper is on *position* estimation. In [9] the backlash size was estimated in the same application and framework as described here.

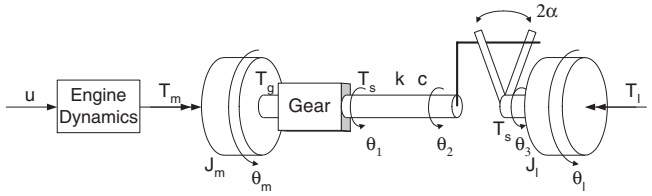

Figure 1: Powertrain model.

One of the filters described here is a continuous Kalman filter with discrete measurement updates at non-equally spaced sampling times. Purely event based sampling of wheel sensors was used in [13].

The data used to evaluate the estimators described in this paper are obtained from simulation of a backlash compensation controller, described in [8]. There, it was assumed that the signals needed for feedback are available directly, from ideal sensors. Also, estimation from measured data is included as evaluation of the final estimator combination. The intention of this paper is to describe the estimators that have to be used when a controller is to be implemented in a vehicle.

The paper is organized as follows: The next section introduces the powertrain system under consideration. In section 3, two estimators for the angular position of a rotating system are described. Estimation of the entire powertrain, including the backlash position is treated in section 4.

2 System models

The following powertrain and backlash models represent the ”true” system, i.e. measurement data is generated from a simulation of this model [8]. The engine and wheel sensor models are then used to generate noisy (quantized) measurement data. The models are also used for the Kalman filters in this paper.

2.1 Powertrain model

The powertrain model is representative for a passenger car on the first gear, at low speed. A two-inertia model is used, where one inertia represents the engine flywheel (*motor*). The other inertia represents the wheels and vehicle mass (*load*). A gearbox is located close to the engine inertia.

The following notation is used, see also Figure 1: The indices m and l refer to motor and load respectively. J_m, J_l [kgm^2] are moments of inertia and b_m and b_l [Nm/(rad/s)] are viscous friction constants. k [Nm/rad] is the shaft flexibility and c [Nm/(rad/s)] is the shaft damping. T_m, T_g, T_s and T_l [Nm] are torques at the engine output, at the gearbox input, at the gearbox output and the load input, and the road load respectively. u [Nm] is the requested engine torque. i [rad/rad] is the gearbox ratio. 2α [rad] is the backlash gap size. θ_m and θ_l [rad] are the angular positions of motor and load. θ_1, θ_2 and θ_3 [rad] are the angular positions of the indicated positions on the shaft. In the sequel, $\hat{}$ will denote an estimated variable.

The equations for the inertias and the gearbox are defined by:

$$J_m\ddot{\theta}_m + b_m\dot{\theta}_m = T_m - T_g \quad (1)$$

$$J_l\ddot{\theta}_l + b_l\dot{\theta}_l = T_s - T_l \quad (2)$$

$$T_g = T_s/i, \theta_3 = \theta_l, \theta_1 = \theta_m/i \quad (3)$$

A flexible shaft with backlash is connecting the gearbox and the load inertia. The shaft torque is modelled as in [12]. This model is more physically correct than the traditionally used dead-zone backlash model. The shaft torque is given by:

$$T_s = k(\theta_d - \theta_b) + c(\omega_d - \omega_b) \quad (4)$$

where $\theta_d \hat{=} \theta_1 - \theta_3 = \theta_m/i - \theta_l$ is the total shaft displacement, and $\theta_b \hat{=} \theta_2 - \theta_3$ is the position in the backlash. With α denoting half the backlash size, the backlash position is governed by the following dynamics:

$$\dot{\theta}_b = \begin{cases} \max(0, \dot{\theta}_d + \frac{k}{c}(\theta_d - \theta_b)) & \theta_b = -\alpha \\ \dot{\theta}_d + \frac{k}{c}(\theta_d - \theta_b) & |\theta_b| < \alpha \\ \min(0, \dot{\theta}_d + \frac{k}{c}(\theta_d - \theta_b)) & \theta_b = \alpha \end{cases} \quad (5)$$

The engine is modelled as an idealised torque generator. Its dynamics is of first order with time constant T_{eng} and time delay L_e:

$$\dot{T}_m = (u(t - L_e) - T_m(t))/T_{eng} \quad (6)$$

The road load is modeled as a random walk process, with v_{T_l} white noise:

$$\dot{T}_l = 0 + v_{T_l} \quad (7)$$

2.2 Speed sensors

The speed sensor used for the ABS system in a vehicle consists of a toothed wheel, which rotates with the same speed as the wheel. A magnetic or optic pick-up senses the passage of the teeth, and generates an oscillating signal with one period per tooth passage. By use of e.g. a Schmidt-trigger, this signal can be transformed into a pulse train. In the ABS system, this signal is filtered and used for speed estimation. In this paper, it is assumed that the pulsating signal is available directly, and counted. The current angular position of the wheel is then calculated as:

$$\theta_l = \frac{2\pi}{N}\#_{\text{pulses}} \quad (8)$$

where N is the number of teeth per revolution and $\#_{\text{pulses}}$ is the value of the pulse counter.

It should be noted that the angular resolution of a typical ABS-sensor is *lower* than the backlash size. In this paper, the used resolution is 0.13 rad, while the backlash size is $2\alpha \approx 0.06$ rad, i.e. a factor 2.25.

The speed sensor for the engine has the same function as the wheel sensors, so a pulsating signal is assumed available here too. However, the resolution of this sensor is better: It has more teeth and, at lower gears, the engine has higher speed than the wheels.

3 Wheel and engine position estimation

In this section, the position of the wheels, θ_l, and the engine, θ_m, are estimated separately. The estimates are then used to calculate the total shaft displacement, which may be of interest, e.g. for control of driveline oscillations (without considering the backlash) [1], [3]. The results presented here are also prerequisites for the estimators in the next section.

The "standard" use of pulse encoders for speed measurement is to count the number of pulses during a *fixed* sampling interval, and then calculate the speed. This approach is too slow for this application, and there will be a quantization error of one pulse in the measurement. Therefore, two alternative estimation methods are described in this section.

3.1 Continuous Kalman filter

In the first filter, the input is assumed to be white noise, v_a, which models jerk as a random walk process. Noise can also be added to the other states. The position measurement, y, used in the simulations is in the form of (8), i.e. a continuous signal with discrete steps. However, in the derivation of the filter, the quantization error is (wrongly) treated as a white noise disturbance, w. This assumption is further dealt with in the next subsection.

$$\dot{\theta} = \omega + v_\theta \quad (9)$$

$$\dot{\omega} = a + v_\omega \quad (10)$$

$$\dot{a} = v_a \quad (11)$$

$$y = \theta + w \quad (12)$$

On state space form:

$$\begin{cases} \dot{x} = Ax + v \\ y = Cx + w \end{cases} \quad (13)$$

where

$$x = \begin{bmatrix} \theta & \omega & a \end{bmatrix}^T, v = \begin{bmatrix} v_\theta & v_\omega & v_a \end{bmatrix}^T \quad (14)$$

$$A = \begin{bmatrix} 0 & 1 & 0 \\ 0 & 0 & 1 \\ 0 & 0 & 0 \end{bmatrix}, C = \begin{bmatrix} 1 & 0 & 0 \end{bmatrix} \quad (15)$$

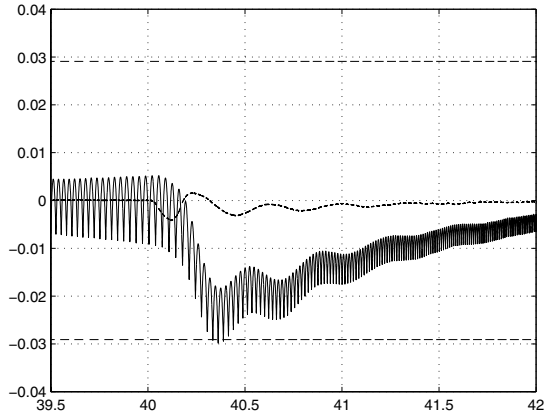

Figure 2: Position estimation error for engine and wheels using separate continuous Kalman filters. As a comparison, the total backlash gap is indicated by the straight horizontal lines. Solid: Wheel position error, $\hat{\theta}_l - \theta_l$. Dashed: Engine position error, scaled with the gear ratio, $(\hat{\theta}_m - \theta_m)/i$.

For this model a Kalman filter is designed:

$$\begin{cases} \dot{\hat{x}} &= A\hat{x} + K(y - C\hat{x}) \\ \hat{y} &= C\hat{x} \end{cases} \tag{16}$$

where K is the Kalman filter gain. The noise covariance matrices Q and R for the process noise, v, and the measurement noise, w, respectively, is chosen as:

$$Q = \begin{bmatrix} 0 & 0 & 0 \\ 0 & 1 & 0 \\ 0 & 0 & 1 \end{bmatrix}, \; R_{\text{engine}} = \rho_m \, , \; R_{\text{wheels}} = \rho_l \tag{17}$$

The simulation of a backlash traverse is shown in Figure 2 and Figure 3. The first figure shows the estimation error for wheel and engine positions. This should be compared to the unfiltered quantization noise with an amplitude of 0.065 rad. The second figure shows the total shaft displacement estimate, which is calculated as $\hat{\theta}_d = \hat{\theta}_m/i - \hat{\theta}_l$.

It can be demonstrated that removal of the acceleration state will result in a stationary estimation error when estimating a constant acceleration.

3.2 Continuous Kalman filter with event based updates

The continuous filter above treats the quantized position signal as continuous with white noise added. If, instead, information about the exact time instants for the pulses is used, a more accurate estimate is expected. This estimation is achieved by an event based sampling method: A continuous wheel/engine model is used for prediction, and discrete position updates are made when a pulse is detected (at non-equal time intervals). The Continuous-Discrete Kalman filter can be formulated as in [6]:

- Pulses arrive at times t_k , $k = 1, \ldots$. At a pulse observation, the system states, $\hat{x}$, and the estimation error covariance matrix, P, are updated according to:

$$\hat{x}_{k|k} = \hat{x}_{k|k-1} + K_{k|k-1}(y_k - C\hat{x}_{k|k-1}) \tag{18}$$
$$P_{k|k} = P_{k|k-1} - K_{k|k-1}CP_{k|k-1} \tag{19}$$

where the Kalman gain, K, is given by:

$$K_{k|k-1} = P_{k|k-1}C^T(CP_{k|k-1}C^T + R)^{-1} \tag{20}$$

- Between the pulse observations ($t_k \leq t < t_{k+1}$), $\hat{x}$ and $P(t)$ evolve continuously from $\hat{x}_{k|k}$ to $\hat{x}_{k+1|k}$ and from $P_{k|k}$ to $P_{k+1|k}$:

$$\dot{\hat{x}} = A\hat{x} \tag{21}$$
$$\dot{P} = AP + PA^T + Q \tag{22}$$

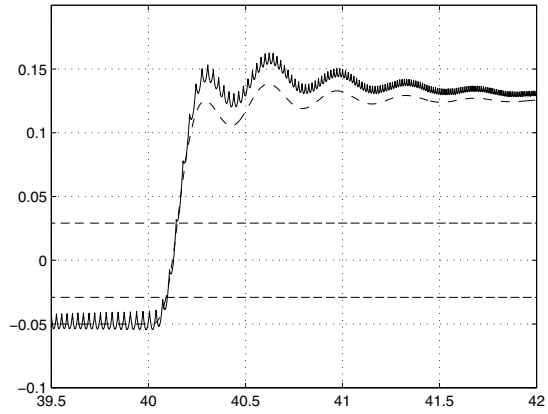

Figure 3: Total shaft displacement estimation using separate Kalman filters for engine position and wheel position. Solid: 3rd order Kalman filter. Dashed: True displacement.

Using the system matrices A, C from (15) and Q, R retuned from (17), the resulting filter performance is radically improved, see Figure 4 for the total shaft displacement estimate, and the estimation error. In Figure 5, the prediction-measurement update process is visualized.

The total shaft displacement, θ_d, can be estimated with high quality. However, there is yet no information about the position in the backlash gap, θ_b. This is treated in the next section.

4 Backlash position estimation

In order to have a good estimate of the backlash position, the backlash has to be included in the model, which will then be nonlinear, and therefore an Extended Kalman filter, EKF, is derived here.

In this paper, the backlash gap size, α, is considered to be a known parameter, which is a fairly strong assumption. In the framework used in this paper, estimation of the backlash size is possible, which is described in [9].

The nonlinear powertrain model can be written as:

$$\begin{cases} \dot{x} = f(x, u, v) \\ y = g(x, w) \end{cases} \tag{23}$$

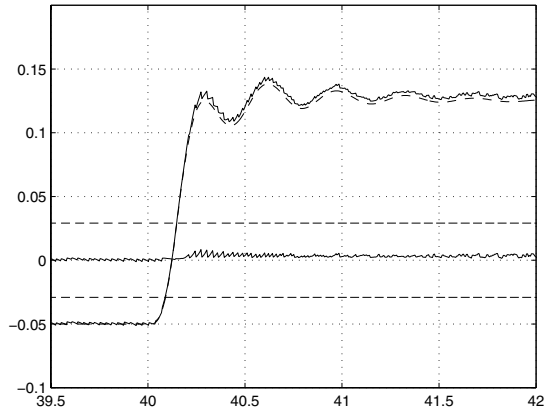

Figure 4: Total shaft displacement estimation using the continuous-discrete estimators on engine and wheels. Solid: Continuous-discrete filter. Dashed: True displacement. The estimation error is also plotted.

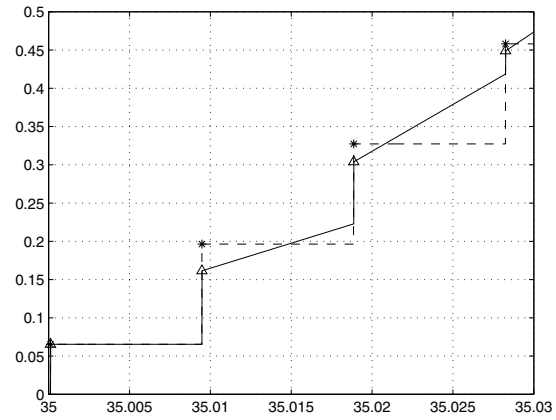

Figure 5: Prediction and measurement updates for the continuous-discrete filter. The plot shows a startup of the filter at $t = 35$ s. Dashed: Continuous quantized signal (used in section 3.1). $*$: Pulse measurements, used in this filter. $\triangle$: Discrete measurement updates (18). Solid: Predicted-updated estimate (18,21).

It will be shown in the sequel that, exploiting the structure of the nonlinear backlash model, the powertrain model can be written as a system switching between two linear modes, called *backlash mode* (bl) and *contact mode* (co). The state-space model (23) can therefore be written as:

$$\dot{x} = \begin{cases} A_{co}x + Bu + v, & \text{co-mode} \\ A_{bl}x + Bu + v, & \text{bl-mode} \end{cases} \quad (24)$$

$$y = Cx + w \quad (25)$$

To derive the A, B, C matrices, the powertrain and backlash models from (1-7) are used.The following state and measurement vectors are used:

$$x = \begin{bmatrix} \theta_m & \omega_m & \theta_l & \omega_l & T_l & T_m & \theta_b \end{bmatrix}^T \quad (26)$$

$$y = \begin{bmatrix} \theta_m & \theta_l \end{bmatrix}^T \quad (27)$$

State and measurement noise vectors are defined as:

$$v = \begin{bmatrix} v_1 & \cdots & v_7 \end{bmatrix}^T, \; w = \begin{bmatrix} w_1 & w_2 \end{bmatrix}^T \quad (28)$$

Using the definitions of the states above, the backlash dynamics (5) can be rewritten as:

$$\dot{\theta}_b = \dot{x}_7 = H(x) \hat{=} \begin{cases} \max(0, h(x)) & x_7 = -\alpha \\ h(x) & |x_7| < \alpha \\ \min(0, h(x)) & x_7 = \alpha \end{cases} \quad (29)$$

where $h(x)$ is linear:

$$h(x) = ax = \begin{bmatrix} k/ci & 1/i & -k/c & -1 & 0 & 0 & -k/c \end{bmatrix} x \quad (30)$$

In the derivation of the Extended Kalman filter, the nonlinear process model (23) is linearized, which in this case is equal to linearizing $H(x)$:

$$a_7 \hat{=} \frac{\partial H}{\partial x} = \begin{cases} 0 & ax < 0 & x_7 = -\alpha & \text{co} \\ a & ax \geq 0 & x_7 = -\alpha & \text{bl} \\ a & & |x_7| < \alpha & \text{bl} \\ 0 & ax > 0 & x_7 = \alpha & \text{co} \\ a & ax \leq 0 & x_7 = \alpha & \text{bl} \end{cases} \quad (31)$$

so the nonlinearity only consists of two distinct modes, each linear.

The seventh row of the A's in (24), a_7, has the value a or 0, depending on the five sets of conditions in (31). A value of a corresponds to the backlash being open (no contact), or in contact, but moving towards opening (bl-mode). A value of 0 corresponds to persistent contact (co-mode).

Since the shaft torque, T_s, shows up in the state equations for ω_m and ω_l, also $\omega_b = \dot{\theta}_b$ does. Therefore the same nonlinearity as in a_7 will also show up in the second and fourth rows of A. Remaining rows of A are equal in both modes, as is B and C, yielding the following matrices:

$$A_{co} = \begin{bmatrix} 0 & 1 & 0 & 0 & 0 & 0 & 0 \\ -\frac{k}{J_m i^2} & -\frac{c/i^2 + b_m}{J_m} & \frac{k}{J_m i} & \frac{c}{J_m i} & 0 & \frac{1}{J_m} & \frac{k}{J_m i} \\ 0 & 0 & 0 & 1 & 0 & 0 & 0 \\ \frac{k}{J_l i} & \frac{c}{J_l i} & -\frac{k}{J_l} & -\frac{c+b_l}{J_l} & -\frac{1}{J_l} & 0 & -\frac{k}{J_l} \\ 0 & 0 & 0 & 0 & 0 & 0 & 0 \\ 0 & 0 & 0 & 0 & 0 & -\frac{1}{T_{eng}} & 0 \\ 0 & 0 & 0 & 0 & 0 & 0 & 0 \end{bmatrix} \quad (32)$$

$$A_{bl} = \begin{bmatrix} 0 & 1 & 0 & 0 & 0 & 0 & 0 \\ 0 & -\frac{b_m}{J_m} & 0 & 0 & 0 & \frac{1}{J_m} & 0 \\ 0 & 0 & 0 & 1 & 0 & 0 & 0 \\ 0 & 0 & 0 & -\frac{b_l}{J_l} & -\frac{1}{J_l} & 0 & 0 \\ 0 & 0 & 0 & 0 & 0 & 0 & 0 \\ 0 & 0 & 0 & 0 & 0 & -\frac{1}{T_{eng}} & 0 \\ \frac{k}{ci} & \frac{1}{i} & -\frac{k}{c} & -1 & 0 & 0 & -\frac{k}{c} \end{bmatrix} \quad (33)$$

$$B = \begin{bmatrix} 0 & 0 & 0 & 0 & 0 & 1/T_{eng} & 0 \end{bmatrix}^T \quad (34)$$

$$C = \begin{bmatrix} 1 & 0 & 0 & 0 & 0 & 0 & 0 \\ 0 & 0 & 1 & 0 & 0 & 0 & 0 \end{bmatrix} \quad (35)$$

A continuous EKF uses a nonlinear process model for prediction, and its linearization for the calculation of K and P. It is formulated as [6]:

$$\dot{\hat{x}} = f(\hat{x}, u) + K(y - h(\hat{x}, u)) \quad (36)$$

$$K = PC(\hat{x})^T R^{-1} \quad (37)$$

$$\dot{P} = A(\hat{x})P + PA(\hat{x})^T - PC(\hat{x})^T R^{-1} C(\hat{x})P + Q \quad (38)$$

In general, an EKF cannot use the stationary solution to the Riccati equation. However, since the model only switches between two linear modes, an EKF based on two stationary linear gains are used here:

$$\dot{\hat{x}} = \begin{cases} A_{co}\hat{x} + Bu + K_{co}(y - C\hat{x}), & \text{co-mode} \\ A_{bl}\hat{x} + Bu + K_{bl}(y - C\hat{x}), & \text{bl-mode} \end{cases} \quad (39)$$

$$\hat{y} = C\hat{x} \quad (40)$$

where K_{co} and K_{bl} are designed for their respective cases, and the A, B, and C-matrices are taken from (32-35). The control signal is delayed with the same time delay as in the engine model, $u(t) = u_{\text{control}}(t - L_e)$.

4.1 Evaluation

The performance of the EKF is evaluated both by simulations and on real vehicle data.

The continuous-discrete filters on wheel and engine, described in section 3.2, are used as pre-filters to the EKF. The inputs to the EKF is therefore $\hat{\theta}_m$ and $\hat{\theta}_l$, the pre-filter estimates, as well as the control signal, u. Figure 6 shows the total shaft displacement estimate, which is improved as compared to Figure 4. The backlash position estimate is seen in Figure 7, where also the influence of the pre-filters is seen. As a robustness check of this filter, it is designed for 1.5 times the nominal values of T_{eng} and L_e.

To further validate the performance of the EKF, measurements in a real vehicle were performed. The measurements were made with high accuracy, and to emulate measurement with lower quality, random errors, simulating sensor tooth position imperfections, were added to the measured signals. The pre-filter - EKF combination had the low quality signals as inputs, and the high quality measurements were taken as the ”true” total shaft displacement. The same signals were also used to simultaneously estimate the backlash gap size, as described in [9]. Figure 8 shows the total shaft displacement estimates and in Figure 9, the backlash position estimate is seen.

5 Conclusions

In this paper, an extended Kalman filter for the backlash position is developed. From the simulations, it is seen that the estimated position follows the true position very well, although some of the model parameters were given with a 50 % error. Evaluation on real vehicle data also shows that the filter works

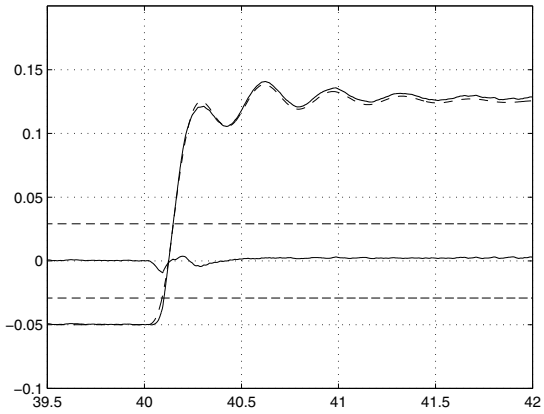

Figure 6: Total shaft displacement. Solid: Extended Kalman Filter estimate (almost on top of true value). Dashed: True displacement. The estimation error is also plotted.

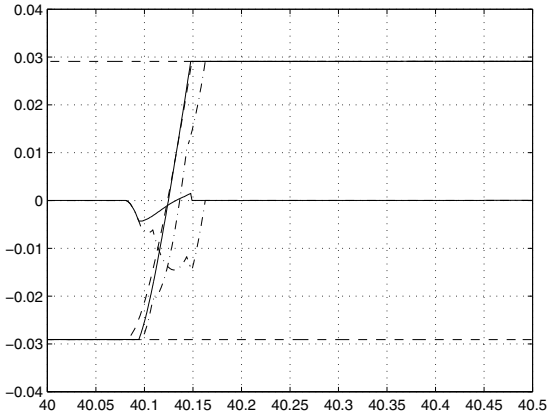

Figure 7: Backlash position estimate. Solid: Extended Kalman Filter estimate (almost on top of true value). Dashed: True value. Dash-dotted: Estimate without pre-filter. The estimation error is also plotted for the two cases.

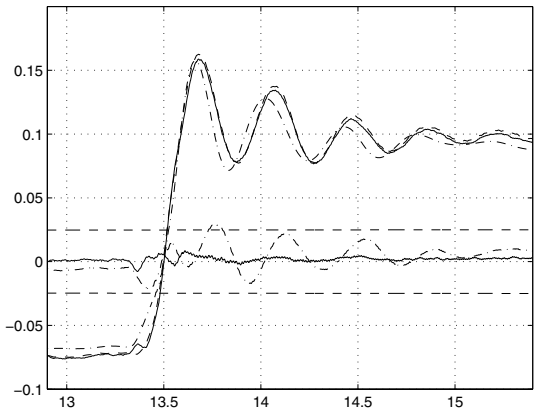

Figure 8: Total shaft displacement with measured data. Solid: Extended Kalman Filter estimate (almost on top of ”true” value). Dashed: ”True” displacement. Dash-dotted: Estimate without pre-filter. The estimation error is also plotted for the two cases (solid and dash-dotted).

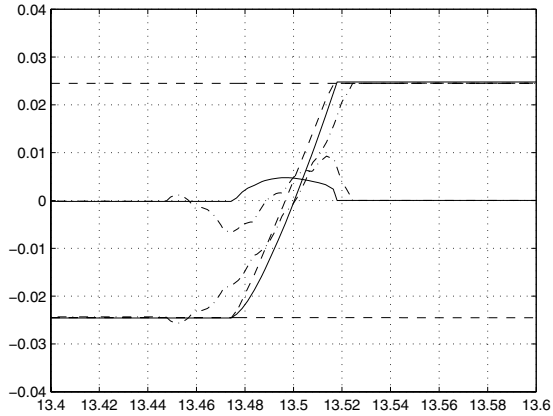

Figure 9: Backlash position estimate with measured data. Solid: Extended Kalman Filter estimate (almost on top of "true" value). Dashed: "True" value. Dash-dotted: Estimate without pre-filter. The estimation error is also plotted for the two cases (solid and dash-dotted).

as expected. Event based Kalman filters for wheel and engine position estimation is also described. These can be used to calculate the total shaft displacement, which can be useful for control of driveline oscillations. By using the position estimators as pre-filters, the backlash position filter performance is improved. The results indicate that the described estimation methods can be useful in powertrain applications, and they may also be applicable to other systems with backlash.

Further application of the estimators to real vehicle data is under investigation.

Use of the estimators in closed loop control for backlash compensation is a natural next step.

Acknowledgements

This work was supported by the Volvo Research and Educational Foundations, the Swedish Automotive Research Program and the Volvo Corporation.

References

[1] J. S. Chen. Active control of torsional vibrations for vehicle drive trains. In *American Control Conference*, pages 1152–1156, Albuquerque, NM, USA, 1997.

[2] Stephen De La Salle, Martin A. Jansz, and Dennis A. Light. Design of a feedback control system for damping of vehicle shuffle. In *EAEC European Automotive Congress*, Barcelona, Spain, 1999.

[3] Jonas Fredriksson, Henrik Weiefors, and Bo Egardt. Powertrain control for active damping of driveline oscillations. *Vehicle Systems Dynamics*, 37(5):359–376, 2002.

[4] K.-V. Hebbale and Y.-A. Ghoneim. A speed and acceleration estimation algorithm for powertrain control. In *American Control Conference*, volume 1, pages 415–420, Boston, MA, USA, 1991.

[5] G. Hovland, S. Hanssen, E. Gallestey, S. Moberg, T. Brogardh, S. Gunnarsson, and M. Isaksson. Nonlinear identification of backlash in robot transmissions. In *33rd International Symposium on Robotics*, Stockholm, Sweden, 2002.

[6] Andrew H. Jazwinski. *Stochastic processes and filtering theory*, volume 64 of *Mathematics in science and engineering*. Academic Press, 1970.

[7] Adam Lagerberg. A literature survey on control of automotive powertrains with backlash. Technical report R013/2001, Control and Automation Laboratory, Department of Signals and Systems, Chalmers University of Techology, December 2001.

[8] Adam Lagerberg and Bo Egardt. Evaluation of control strategies for automotive powertrains with backlash. In *AVEC '02, Intl. Symp. on Advanced Vehicle Control 2002*, Hiroshima, Japan, 2002.

[9] Adam Lagerberg and Bo Egardt. Estimation of backlash with application to automotive powertrains. In *IEEE Conference on Decision and Control, Submitted*, Hawaii, 2003.

[10] Mattias Nordin and P. Bodin. A backlash gap estimation method. In *European Control Conference*, volume 4, pages 3486–91, Rome, Italy, 1995.

[11] Mattias Nordin, P. Bodin, and P.-O. Gutman. New models and identification methods for backlash and gear play. In Gang Tao and Frank L. Lewis, editors, *Adaptive Control of Nonsmooth Dynamic Systems*, pages 1–30. Springer, 2001.

[12] Mattias Nordin, J. Galic, and P.-O. Gutman. New models for backlash and gear play. *International Journal of Adaptive Control and Signal Processing*, 11:49–63, 1997.

[13] Niclas Persson. *Event Based Sampling with Application to Spectral Estimation*. Licentiate thesis, Linkoping University, 2002.

[14] Jae-Yoo Yoo, Tae-Sik Park, Seong-Hwan Kim, Nam-Jeung Kim, and Ji-Yoon Yoo. Speed estimation of an IM using kalman filter algorithm at ultra-low speed region. In *1997 IEEE International Electric Machines and Drives Conference*, pages MC2/4.1–3, Milwaukee, WI, USA, 1997.